

, 72, . . . , 49010, ; e-mail: decinpix@gmail.com

++

gnuplot.

40 %.

This paper presents the results of mathematical modeling of non-stationary temperature fields in a typical solar panel under real environmental conditions. The mathematical model is based on a system of nonlinear ordinary differential equations with corresponding initial and boundary conditions. The model takes into account radiation losses from the surface of the panel, which are determined by the Stefan–Boltzmann law, and convective losses due to free and forced convection. The solar flux density was considered constant, but its value depended on the solar panel setting angle. The temperature dependence of the solar cell efficiency was calculated using a standard method. A computational algorithm was developed in C++ using standard mathematical libraries with a linearization of the system of ordinary differential equations. The results were visualized using the gnuplot graphing utility. The temperature distribution in each of the solar panel layers was obtained as a function of the ambient temperature. It was found that an increase in the ambient temperature leads to a significant decrease, up to 40%, in the solar panel efficiency. With increasing ambient temperature, the time of transition to steady operation increases. The solar panel temperature was related to the blackness degree of the protective glass. It was shown that in the Kirchhoff approximation it is necessary that the blackness degree of the selective coating of the protective glass be a maximum, which reduces the temperature of the system and increases its efficiency. The solar panel temperature was related to the wind speed. It was shown that the convective losses increase with the wind speed, which has a favorable effect on the solar panel temperature regime. The results of the study showed the effect of various external environmental factors on the temperature regime of a solar panel and a way to maximize its efficiency by optimizing its parameters. The results may be used in the development and production of improved solar panels with minimum temperature effects on their efficiency.

Keywords: *non-stationary mathematical model, system of nonlinear differential equations, numerical experiments, silicon solar panel, solar panel efficiency.*

[1].

[2].

[3].

[4 – 9]. [4]

1000 / ².

15° 50° .

~2 %.

[5],

1000 / ²,

~2 %

25° 60° [6]. [7]

33° 56°

5 %

), (

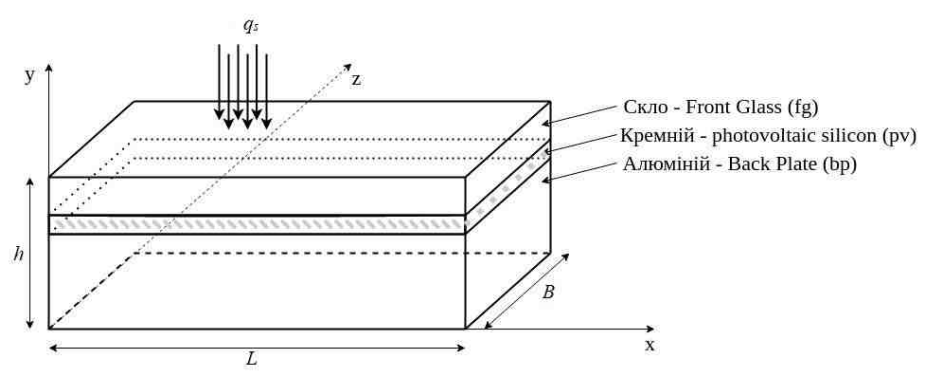
[9]

1 / 5 / .

[10].

[11 – 13].

3-
 ++
 .1
 .1
 h, L, B -
 q_s - / 2 .



. 1 -

:

$$\rho_{fg} h_{fg} C_{fg} \frac{dT_{fg}}{dt} = \alpha_{fg} (T_a - T_{fg}) + F_{fgsky} (T_{sky}^4 - T_{fg}^4) + F_{fggro} (T_{gro}^4 - T_{fg}^4) + \frac{\lambda_{fg}}{h_{fg}} (T_{pv} - T_{fg}) + q_1, \quad (1)$$

:

$$\rho_{pv} h_{pv} C_{pv} \frac{dT_{pv}}{dt} = \frac{\lambda_{pv}}{h_{pv}} (T_{fg} - T_{pv}) + \frac{\lambda_{pv}}{h_{pv}} (T_{bg} - T_{pv}) + q_2, \quad (2)$$

:

$$\rho_{bg} h_{bg} C_{bg} \frac{dT_{bg}}{dt} = \alpha_{bg} (T_a - T_{bg}) + F_{bgsky} (T_{sky}^4 - T_{bg}^4) + F_{bggro} (T_{gro}^4 - T_{bg}^4) + \frac{\lambda_{bg}}{h_{bg}} (T_{pv} - T_{bg}), \quad (3)$$

h_{fg}, h_{pv}, h_{bg} — thermal conductivities of the film, the glass, and the substrate, respectively; $\rho_{fg}, \rho_{pv}, \rho_{bg}$ — densities of the film, the glass, and the substrate, respectively; C_{fg}, C_{pv}, C_{bg} — specific heats of the film, the glass, and the substrate, respectively; α_{fg}, α_{bg} — coefficients of convective heat transfer from the ambient air to the film and from the ambient air to the substrate, respectively; $\lambda_{fg}, \lambda_{pv}, \lambda_{bg}$ — thermal conductivities of the film, the glass, and the substrate, respectively; q_1, q_2 — heat fluxes from the film and from the glass to the substrate, respectively; $F_{fgsky}, F_{fggro}, F_{bgsky}, F_{bggro}$ — view factors from the film to the sky, from the film to the ground, from the glass to the sky, and from the glass to the ground, respectively.

$$F_{fgsky} = \frac{1}{2} (1 + \cos \beta), \quad (4)$$

$$F_{fggro} = \frac{1}{2} (1 - \cos \beta), \quad (5)$$

$$F_{bgsky} = \frac{1}{2} (1 + \cos(\pi - \beta)), \quad (6)$$

$$F_{bggro} = \frac{1}{2} (1 - \cos(\pi - \beta)), \quad (7)$$

β — angle between the normal to the film surface and the direction of the sun rays, $\beta = 45^\circ$.

$$q_1 = a_{fg} q_s, \quad (1)$$

:

$$q_1 = a_{fg} q_s, \quad (8)$$

a_{fg} —

$$q_2 = a_{pv} q_s, \quad (2)$$

:

$$q_2 = a_{pv} \tau_{fg} q_s - \frac{P_{pv}}{A}, \quad (9)$$

$$a_{pv} = \frac{\tau_{fg}}{A} \left(\frac{P_{pv}}{q_s} + A \right), \quad (10)$$

$$P_{pv} = \gamma q_s A, \quad [9]:$$

$$= \frac{P_{ref}}{A} \left[1 - \beta_0 (T_{pv} - T_{ref}) + \log(q_s) \right], \quad (10)$$

$$T_{ref} = 303, 15 \text{ K}; \quad \beta_0 = 1/K; \quad \gamma = \dots$$

(1) – (10)

odeint,

$$(1) \quad (3),$$

$$[14].$$

$$(T_{sky}^4 - T_{fg}^4) = (T_{sky}^2 + T_{fg}^2)(T_{sky} + T_{fg})(T_{sky} - T_{fg}), \quad (11)$$

$$(T_{gro}^4 - T_{fg}^4) = (T_{gro}^2 + T_{fg}^2)(T_{gro} + T_{fg})(T_{gro} - T_{fg}), \quad (12)$$

$$(T_{sky}^4 - T_{bg}^4) = (T_{sky}^2 + T_{bg}^2)(T_{sky} + T_{bg})(T_{sky} - T_{bg}), \quad (13)$$

$$(T_{gro}^4 - T_{bg}^4) = (T_{gro}^2 + T_{bg}^2)(T_{gro} + T_{bg})(T_{gro} - T_{bg}), \quad (14)$$

\tilde{T} –

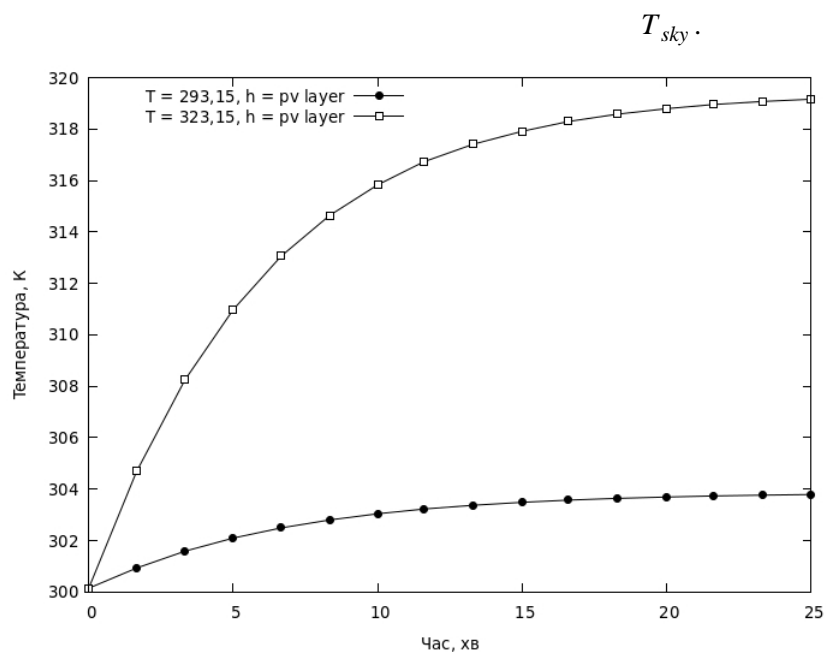
(1) – (3)

$$T_0 = 303, 15 \text{ K} \quad [15].$$

gnuplot [16].

T_{sky}	303,15		
T_{gro}	283,15	,	-
y_{ref}	13	,	-
$\dots fg, \dots pv, \dots bp$	3000, 2330, 3000		/ ³
$C_{fg}, C\rho_{pv},$ $C\rho_{bp}$	500, 677, 500		/
	0,9		
$a_{fg}, a_{bg},$	0,96; 0,9		
τ_{fg}	0,95		
$\lambda_{fg}, \lambda_{pv}, \lambda_{bg},$	1,8; 130, 1,8		/
q_{fg}	1000		/
w	3,2		/
h	0,04		
L	1,04		
B	0,46		

. 2



. 2 -

. 2

15

320

T_{sky}

15 .
4 %,

$$T_{sky} = 323,5 \hat{E} - 8,5 \%$$

$$T_{sky} = 293,5 \hat{E}$$

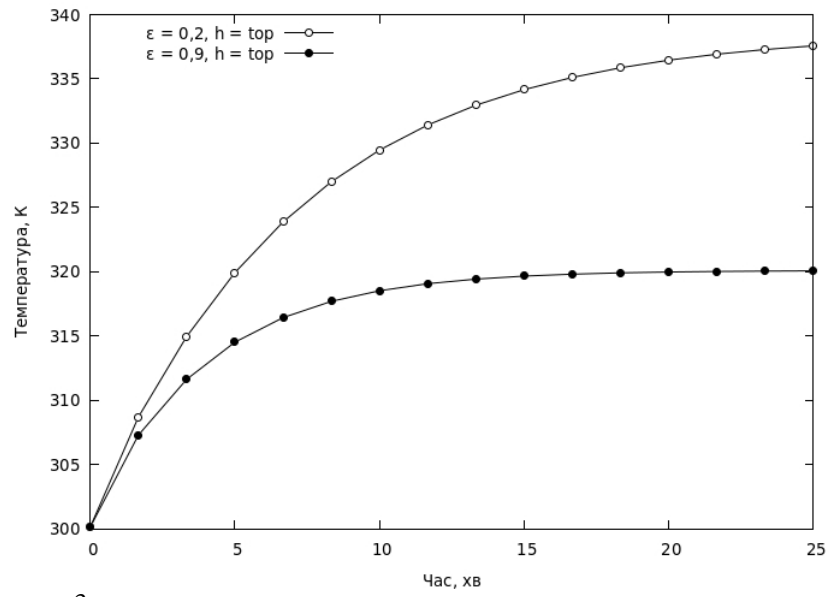
12,

40 %,

. 3

. 3

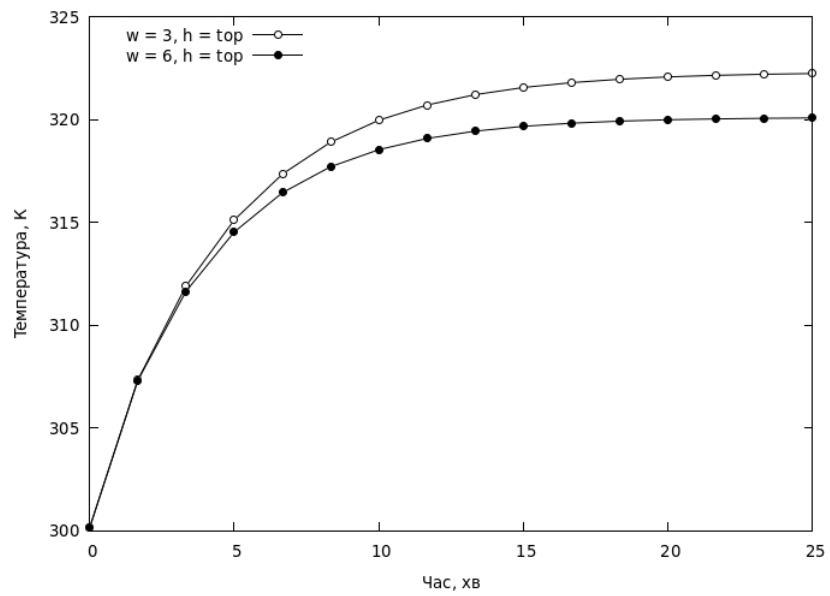
ϵ



. 3 -

. 4

(3 / - 6 /)



. 4 -

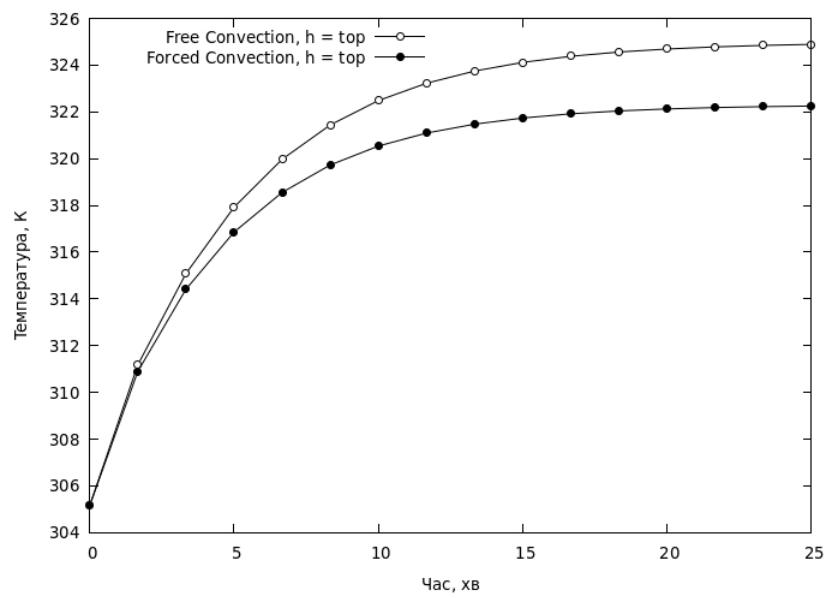
. 5

$$T_{sky} = 303,15 \hat{E} .$$

. 5

[11].

7 , ,



. 5 -

++

gnuplot

40 %.

1. . 2021. 2. 3–19. <https://doi.org/10.15407/itm2021.02.003>
2. . 2021. 2. . 100–106. <https://doi.org/10.15407/itm2021.02.100>
3. *Singh G. K.* Solar power generation by PV (photovoltaic) technology. A review: Energy. 2013. V. 53. P. 1–13. <https://doi.org/10.1016/j.energy.2013.02.057>
4. *Tobnaghi D. M., Madatov R., Naderi D.* The Effect of Temperature on Electrical Parameters of Solar Cells. International Journal of Advanced Research in Electrical, Electronics and Instrumentation Engineering. 2013. V. 2. P. 6404–6407
5. *Khalis M., Masrour R., Khrypunov G., Kirichenko M., Kudy D., Zazoui M.* Effects of Temperature and Concentration Mono and Polycrystalline Silicon Solar Cells: Extraction Parameters. Journal of Physics: Conference Series. 2015. V. 758. P. 758. <https://doi.org/10.1088/1742-6596/758/1/012001>
6. 2020. 3(62). . 35–41.
7. *Famaz A., Aziz A. S., Shukor M., Farudun M.* Fundamental study on the impacts of water-cooling and accumulated dust on photovoltaic module performance. International Journal of Power Electronics and Drive Systems. 2022. V. 13. P. 2421–2431. <https://doi.org/10.11591/ijpeds.v13.i4.pp2421-2431>
8. *Skoplaki E., Palyvos J. A.* On the temperature dependence of photovoltaic module electrical performance. A review of efficiency/power correlations. Solar Energy. 2009. V. 83. P. 614–624. <https://doi.org/10.1016/j.solener.2008.10.008>
9. *Soliman A. S., Dong L. Xu, J., Cheng P.* Numerical investigation of a photovoltaic module under different weather conditions. Energy Reports. 2022. V. 8. P. 1045–1058. <https://doi.org/10.1016/j.egyr.2022.10.348>
10. *Notton G., Cristofari C., Mattei M., Poggi P.* Modelling of a double-glass photovoltaic module using finite differences. Applied Thermal Engineering. 2005. V. 25. P. 2854–2877. <https://doi.org/10.1016/j.applthermaleng.2005.02.008>
11. 2022. 34. . 48–58.
12. XXIV “ ”, 2022 ., . 99.
13. “ ”, 23-25 2022 ., . 90.
14. *Serrano E. S.* Differential Equations: Applied Mathematical Modeling, Nonlinear Analysis, and Computer Simulation in Engineering and Science. HydroScience Inc. 2016. P. 60.
15. *Sauer T.* Numerical Analysis. Pearson. 2011. V.2. P. 427.
16. GNUplot. URL: <http://www.gnuplot.info> (02.05.2023).

13.06.2023,
13.09.2023